Influence of Uncertainties in the Material Properties of Brain Tissue on the Probabilistic Volume of Tissue Activated

Christian Schmidt*, *Student Member, IEEE*, Peadar Grant, *Member, IEEE*, Madeleine Lowery, *Member, IEEE*, and Ursula van Rienen, *Member, IEEE*

***Abstract*—The aim of this study was to examine the influence of uncertainty of the material properties of brain tissue on the probabilistic voltage response and the probabilistic volume of tissue activated (VTA) in a volume conductor model of deep brain stimulation. To quantify the uncertainties of the desired quantities without changing the deterministic model, a nonintrusive projection method was used by approximating these quantities by a polynomial expansion on a multidimensional basis known as polynomial chaos. The coefficients of this expansion were computed with a multidimensional quadrature on sparse Smolyak grids. The deterministic model combines a finite element model based on a digital brain atlas and a multicompartmental model of mammalian nerve fibers. The material properties of brain tissue were modeled as uniform random parameters using data from several experimental studies. Different magnitudes of uncertainty in the material properties were computed to allow predictions on the resulting uncertainties in the desired quantities. The results showed a major contribution of the uncertainties in the electrical conductivity values of brain tissue on the voltage response as well as on the predicted VTA, while the influence of the uncertainties in the relative permittivity was negligible.**

***Index Terms*—Deep brain stimulation (DBS), finite element methods (FEMs), neural response, sensitivity analysis.**

I. Introduction

THE neurosurgical method deep brain stimulation (DBS) has evolved as a widely employed procedure to treat the symptoms of motor skill disorders such as Parkinson's disease (PD), essential tremor, and dystonia [1]. In a stereotactic surgery, a stimulation electrode is implanted in deep brain areas, which are then stimulated by electrical pulses to improve the symptoms. Since the early 1990s, DBS electrodes from the vendor Medtronic were implanted and used to treat symptoms of motor skill disorder in approximately 70 000 patients worldwide [2]. The DBS stimulation pulses commonly applied in the DBS therapy in humans are voltage-controlled square-wave signals. In addition to voltage-controlled stimulation, current-controlled stimulation is now also available. To date, current-controlled stimulation has been employed mostly in animal studies, but is attracting increasing interest in human DBS, due to the greater stability in current delivered and potential to reduce unwanted side effects that it offers [3]. Although successfully employed across various clinical fields, the fundamental mechanisms of the action of DBS remain uncertain [4].

Starting in the last decade, many computational models to gain insight into these mechanisms have been developed. A number of these models have concentrated on the computation of the neural activation by using neuron models in combination with finite element methods (FEMs) to estimate the voltage response for a certain DBS stimulation pulse in the proximity of the stimulated target [5]–[8]. The extent of the computed volume of tissue activated (VTA) varies substantially with the material properties of the surrounding brain tissue [6]. The values for the material properties of brain tissue in such volume conductor models are typically based on experimental data, which vary widely in the literature [9]–[12]. The measurement of the material properties is made challenging not only by interfering effects, such as electrode polarization at low frequencies, but also difficulties associated with measuring material properties *in vivo* or *in vitro*. Therefore, literature values are scarce, especially for frequencies below 1 MHz, and are based either on experiments carried out on live tissue or on excised tissue, which is known to be subject to uncertainty compared to live tissue [13]. Present computational models, therefore, cover only some possible cases of the resulting voltage response and extent of the neural activation in DBS, and do not consider the uncertainty in these quantities. This additional information on the probability distribution of the extent of neural activation could help engineers as well as clinicians in evaluating the actual activated area and rating the likelihood of undesired activation. To investigate the influence of the uncertainty in the material properties on the uncertainty in the voltage response and the VTA, a standard approach would be to compute the desired quantities for a certain amount of different samples of the material properties and evaluate the stochastics of the desired quantities. This approach, known as Monte Carlo simulation (MCS), has the major disadvantage that the variance of the desired quantities converges relatively slowly with an asymptotical convergence

Manuscript received November 16, 2012; revised December 16, 2012; accepted December 17, 2012. Date of publication December 20, 2012; date of current version April 15, 2013. This work was supported by the DFG (German Science Foundation) Research Training Group 1505/1 "welisa." *Asterisk indicates corresponding author*.

*C. Schmidt is with the Institute of General Electrical Engineering, University of Rostock, Rostock 18059, Germany (e-mail: christian.schmidt6@uni-rostock.de).

P. Grant and M. Lowery are with the School of Electronics, Electrical and Communications Engineering, University College Dublin, Dublin 4, Ireland (e-mail: peadar.grant@ucd.ie; madeleine.lowery@ucd.ie).

U. van Rienen is with the Institute of General Electrical Engineering, University of Rostock, Rostock 18059, Germany (e-mail: ursula.van-rienen@uni-rostock.de).

Digital Object Identifier 10.1109/TBME.2012.2235835

rate of $1/\sqrt{N}$ for a number N of samples, thereby requiring a large number of samples to acquire sufficient accuracy [14]. The MCS is, thus, only marginally applicable for volume conductor models of DBS, since the deterministic model is computationally costly with up to several million unknowns. As an alternatively approach to obtain the stochastics of the desired quantities in a reasonable time, they can be approximated by a polynomial expansion in random variables. This approach, known as polynomial chaos (PC), can be classified into an intrusive approach, in which the PC is incorporated into the deterministic code to form a probabilistic version of it, and a nonintrusive approach, in which the deterministic code remains unchanged and is used similar to a "black-box." Although the nonintrusive PC methods are well established in various modeling fields of bioengineering, such as biomechanics [15] and drug concentration estimation [16], the applications in electrical bioengineering are still scarce. The major advantage of this method is that the deterministic model is only required for the computation of the coefficients of the polynomial expansion, which can be achieved by using stochastic collocation [15] or spectral projections [17]. The nonintrusive PC replaces an existing MCS by a surrogate model, which differs from a classical MCS only by the choice of nonrandom samples for the deterministic model evaluation and, therefore, also accounts for nonlinearities [18].

The aim of this study is the application of the nonintrusive spectral projection method to a volume conductor model of DBS to quantify the uncertainties in the voltage response and VTA. The integrals resulting out of the computation of the expansion coefficients are evaluated numerically by using multidimensional quadrature on Smolyak sparse grids [19]. The volume conductor model used in this study consists of an idealized heterogeneous anatomical human brain and is based on segmented magnetic resonance imaging (MRI) data of a digital brain atlas [20], [21]. A realistic model of the Medtronic DBS electrode Mo. 3387 expanded by a peri-electrode space was incorporated into the model and positioned in the subthalamic nucleus (STN) [8], which is a common target in DBS for the treatment of the symptoms of PD [22]. The time-dependent voltage response in the proximity of the active electrode contact was computed for common voltage-controlled and current-controlled DBS pulses using the Fourier FEM method in combination with equivalent circuits. A multicompartmental mammalian nerve fiber model was used to compute the threshold amplitudes for axons in the proximity of the active electrode contact and the resulting VTA [6], [23]. The uncertainty in the voltage response and the VTA was computed for different sets of probabilistic parameters, where the conductivity and relative permittivity were investigated separately as well as in combination. The uncertainty quantification of the voltage response and VTA can be obtained by the combination of these parameters, while the separate investigation allowed a sensitivity analysis of the voltage response and VTA on each of these parameters.

II. Methods

A. Uncertainty Quantification

Uncertainty quantification is a method to investigate the influence of uncertainty in the M random model parameters $X_1, \ldots, X_M$, which are assumed to be independent, on a desired quantity Z of the model. To compute the probability density of the quantity Z, a nonintrusive projection method was implemented, as described by Eldred *et al*. [24], and is outlined briefly in the following section. The quantity Z is expanded on a basis of multivariate orthogonal polynomials ψ_i

$$Z = \sum_{i=0}^{\infty} c_i \psi_i(\boldsymbol{\xi}) \tag{1}$$

which are dependent on the multivariate random variables $\boldsymbol{\xi} = (\xi_1, \ldots, \xi_M)$ with uniform distributions $\mathcal{U}[-1, 1]$. The optimal basis polynomials are formed by the product of the 1-D Legendre polynomials $P_n(x)$, for which the probability density function $f(\boldsymbol{\xi})$ of the random variables $\boldsymbol{\xi}$ and the weighting function $w(x)$ of the inner product $\langle ., . \rangle$ differ only by a constant factor in $[-1, 1]$. In practice, the expansion in (1) is truncated for a number of basis polynomials $P_{\mathsf{out}} + 1$

$$Z \approx \sum_{i=0}^{P_{\mathsf{out}}} c_i \psi_i(\boldsymbol{\xi}) \tag{2}$$

where P_{out} is determined by the maximal expansion degree p

$$P_{\mathsf{out}} + 1 = \sum_{i=0}^{p} \binom{M+i-1}{i} = \binom{M+p}{p}. \tag{3}$$

The coefficients c_i are determined by projecting the truncated expansion of Z on each basis polynomial and exploiting its orthogonality in the domain $\Omega = [-1, 1]^M$:

$$c_j = \frac{1}{\langle \psi_j(\boldsymbol{\xi}), \psi_j(\boldsymbol{\xi}) \rangle} \int_{\Omega} Z(\boldsymbol{\xi}) \psi_j(\boldsymbol{\xi}) f(\boldsymbol{\xi}) \, \mathsf{d}\boldsymbol{\xi} \tag{4}$$

with $j = 0, 1, \ldots, P_{\mathsf{out}}$. Since the quantity Z depends on the parameters $X_1, \ldots, X_M$, a transformation has to be defined, mapping the uniform random variable ξ_i on the random variable X_i

$$X_i = \mathcal{T}_i(\xi_i) = G^{-1}(F(\xi_i)), \quad i = 1, \ldots, M \tag{5}$$

where G is the cumulative distribution function (CDF) of the random parameter X_i and F is the CDF of ξ_i [25]. This transformation $\mathcal{T}_i$ exists, if the CDF G is continuous and strictly monotonically increasing, which is the case in this study. While the denominator in (4) can be computed analytically, the integral in the nominator is computed by a numerical evaluation using a multidimensional cubature. The nodes and weights for the numerical evaluation of the integral are obtained using Smolyak sparse grids $S(L, M)$, as described by Nobile *et al*. [19], in combination with the 1-D Clenshaw–Curtis quadrature. The nodes t_i of the Clenshaw–Curtis quadrature correspond to the roots of the nth Chebyshev polynomial and become nested, if n is chosen as

$$n := n(l) = \begin{cases} 2^l + 1, & \text{if } l \in \mathbb{N}_+ \\ 1, & \text{if } l = 0 \end{cases} \tag{6}$$

where l is the level of the 1-D Clenshaw–Curtis quadrature. The nodes and weights of the Clenshaw–Curtis rule were computed using an algorithm based on a fast Fourier transform (FFT) [26]. The Smolyak sparse grid $S(L, M)$ is a combination of tensor

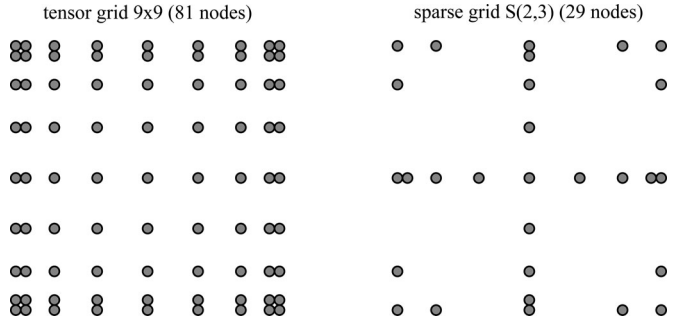

Fig. 1. Nodes of a 2-D 9×9 tensor grid and a corresponding level 3 Smolyak sparse grid $S(2,3)$.

grids, where the sum of the levels $l_1, \ldots, l_M$ is smaller or equal to the grid level L (see Fig. 1). For the computation of the coefficients c_j in (4) and, therefore, the computation of the approximation of the quantity $Z(X_1(\xi_1), \ldots, X_M(\xi_M))$, the deterministic model needs to be evaluated for the nodes $\boldsymbol{t}^{(i)} = (t_1^{(i)}, \ldots, t_M^{(i)})$ of the sparse grid with $i = 1, \ldots, N$, where N is the number of nodes. The numerical evaluation of the nominator in (4) is then expressed by

$$\langle Z(\boldsymbol{\xi}), \psi_j(\boldsymbol{\xi}) \rangle \approx \sum_{i=1}^{N} Z\left(X_1\left(t_1^{(i)}\right), \ldots, X_M\left(t_M^{(i)}\right)\right) \times \psi_j(\boldsymbol{t}^{(i)}) \cdot w^{(i)} \tag{7}$$

where $w^{(i)}$ is the product of the corresponding 1-D weights. In a preliminary study, the nonintrusive PC approach was validated in a simple 2-D finite element model, which allowed a large number of deterministic model evaluations in a reasonable time [27]. Results computed with the proposed approach were in good agreement with that computed with MCS. To quantify the magnitude of uncertainty in the parameters X_i and the quantity Z, the relative standard deviation σ_r

$$\sigma_r = \frac{\sigma}{\mu} \tag{8}$$

with the mean μ and the standard deviation σ is used. The 0.025 and 0.975 quantiles are used to illustrate the confidence interval.

B. Electrical Properties of Brain Tissue

The electrical properties of brain tissue form the random parameters X_i described in the previous section. The values for the conductivity and relative permittivity of gray matter and white matter are based on values from a series of studies reported in the literature [9]–[12]. These values are reported at different frequencies, but for the volume conductor model these values are required at a frequency of 2 kHz. Since the frequency-dependent material properties of gray matter and white matter are only available for a wide range of frequencies in [9], the conductivity values in the other studies were approximated at this frequency by dividing the conductivity value obtained from each of these studies by the conductivity value obtained from [9] at the appropriate frequency and multiplying it with the conductivity value obtained from [9] at 2 kHz (see Table I). Since no information on the distribution of the values is presently available, a uniform distribution was assumed with lower and upper boundaries according to the determined conductivity values. The uncertainty in the relative permittivity was modeled by applying the same uncertainty to the relative permittivity of Gabriel *et al*. [9]. In addition to areas of gray and white matter in the brain, several areas contain out of cerebrospinal fluid, which was assigned a conductivity value of 2 Sm^{-1} and a relative permittivity of 200 [9]. Due to the tissue-implant reaction, a thin encapsulation layer is formed surrounding the electrode body. Likewise for the other brain tissues, the electrical properties of this encapsulation layer are subject to uncertainty. Since the focus was on the investigation of the influence of uncertainty in the conductivity and relative permittivity of brain tissues, the material properties of the encapsulation layer were not investigated separately, but were modeled as a function of the uncertainty in the material properties of brain tissue. To model the chronic stage, in which the encapsulation is characterized by a higher resistivity than the surrounding brain tissue, the conductivity and the relative permittivity of the encapsulation layer were approximated to be half value of the uncertain conductivity of gray matter [5], and the uncertain relative permittivity of brain tissue [8], respectively. The conductivities of gray matter and white matter were modeled as uniform distributions with a relative standard deviation σ_r of 10%, 20%, and 40% (see Table II). To investigate the influence of the relative permittivity, an uncertainty of 20% was applied on the relative permittivity values of Gabriel *et al*. [9].

TABLE I
CONDUCTIVITY VALUES FOR GRAY AND WHITE MATTER AT A FREQUENCY OF 2 KHZ: [1] [9], [2] [10] SCALED, [3] [12] SCALED, [4] AND [11] SCALED

white matter $[\mathrm{S\,m^{-1}}]$	**gray matter** $[\mathrm{S\,m^{-1}}]$
0.064^1	0.103^1
0.138^2	0.237^2
0.211^3	0.229^3
0.375^4	0.538^4

TABLE II
UPPER BOUNDARIES a, LOWER BOUNDARIES b, MEAN μ, AND RELATIVE STANDARD DEVIATION σ_r OF THE UNIFORM DISTRIBUTIONS OF THE CONDUCTIVITY AND RELATIVE PERMITTIVITY OF WHITE MATTER AND GRAY MATTER

	conductivity $[\mathrm{S\,m^{-1}}]$			**relative permittivity**			σ_r [%]
	a	b	μ	a	b	μ	
white matter	0.064	0.091	0.078			40,234	10
	0.064	0.132	0.098	26,297	54,171	40,234	20
	0.064	0.353	0.209			40,234	40
gray matter	0.103	0.146	0.125			93,983	10
	0.103	0.212	0.158	61,426	126,540	93,983	20
	0.103	0.568	0.336			93,983	40

C. Finite Element Model

An idealized finite element model of the human brain was developed, based on the data of the digital SRI24 multichannel brain atlas [20]. The model comprises heterogeneous tissue properties of gray matter, white matter, and cerebrospinal fluid, which were derived from the segmented magnetic

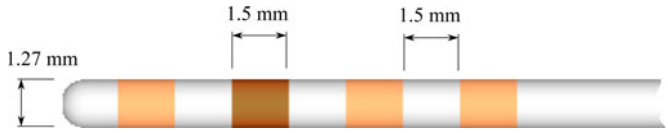

Fig. 2. Representation of the Medtronic DBS electrode Mo. 3387. The cylindrical electrode has four electrode contacts positioned equidistantly at the tip of the electrode lead. The second electrode contact is used for unipolar stimulation.

resonance images of the digital brain atlas. A realistic model of the Medtronic DBS electrode Mo. 3387 (see Fig. 2) surrounded by a 2-mm thick encapsulation layer was incorporated into the model with the second electrode contact located in the stimulated target area. This area and the electrode tip is enclosed by a region of interest (ROI) with an edge length of 19 mm. The mesh was manually refined until the deviation in the integral of the current density over the second electrode contact was below 1% resulting in approximately $1.4 \cdot 10^6$ mesh elements. A more detailed description of the brain model can be found in [21]. Unipolar stimulation was applied by setting the second electrode contact as active, while the remaining electrode contacts were set to a floating potential, i.e., no net current flow occurring through their surface. The electrical ground reference was defined on a circular plane located at the bottom of the brain model. To compute the voltage distribution ϕ and current I in the brain model, Laplace's equation

$$\nabla \left[(\kappa + \mathrm{j}2\pi f \varepsilon) \nabla \phi \right] = 0 \tag{9}$$

which applies for conductive κ and capacitive ε tissue properties was solved at a frequency of $f = 2$ kHz. For voltage-controlled stimulation, constant potentials were applied to the active electrode contact and ground using Dirichlet boundary conditions, while the remaining exterior boundaries were set to be insulating using Neumann boundary conditions. For current-controlled stimulation, a normal current density was applied to the active electrode contact. The FEM computations were carried out with the commercial software COMSOL MULTIPHYSICS (v4.2, COMSOL AG) using quadratic elements and the generalized minimal residual method with a geometric multigrid preconditioner. The iteration was stopped when the norm of the residual was below 1×10^{-6}.

D. Waveform Computation

Common square-wave-shaped DBS pulses with a frequency of 130 Hz and a pulse width of 60 μs were used. The modeled DBS pulse is monophasic and would not produce a charge-balanced stimulation over time. Since the threshold computation in the axon model is mainly influenced by the stimulus amplitude [6], a charge-balancing period with an amplitude substantially smaller than the stimulus pulse amplitude would most likely have no effect on the computation of the VTA. To compute the time-dependent voltage response, a method based on the Fourier FEM method, was implemented [28]. In this method, the DBS pulse is transformed into the frequency domain using an FFT, scaled and phase shifted by the transfer function obtained from the finite element model at each location of interest in the proximity of the stimulated target, and transformed back into the time domain using an inverse FFT. Instead of computing the components of the transfer function for each harmonic frequency of the DBS pulse in the frequency domain, an equivalent circuit model comprising the tissue resistance R_t and tissue capacitance C_t is used to obtain the transfer function of the finite element model at each observation point. The resistance R_t and capacitance C_t are derived from the surface integral of the current density over the active electrode contact. This method allows the computation of the voltage response in the tissue with only one evaluation of the FEM model. The effects at the electrode-tissue interface are modeled by a constant phase element as described by Grant and Lowery [6]. It is assumed that the effects of the electrode-tissue interface can be modeled by the constant phase element for frequencies above 130 Hz, in agreement with the results of an experimental study [29]. Moreover, the constant phase element is negligible for current-controlled stimulation, since capacitive and dispersive effects dominate the waveform shape [6].

E. Computation of the VTA

The generalized mammalian axon model developed by McIntyre *et al.* [23] was used to determine the extent of the region of neural activation surrounding the electrode. Axons were arranged in a rectangular 7×18 grid, with a spacing of 0.5 mm in the x- and y-directions normal and parallel to the electrode's central axis, respectively. The fibers were parallel to the z-axis, with identical z-coordinates on all fibers. Each axon comprised 21 nodes of Ranvier with an internodal spacing of 500 μm. The fiber diameter was set to 5.7 μm, with all dependent parameter values set equal to those given in [23]. The model was implemented using NEURON 7.1 in conjunction with the Python interpreter [30].

For each axon, the voltage at each of the 21 nodes in response to a 1 V (voltage controlled) and 1 mA (current controlled) stimulus at the DBS electrode contact was calculated using the finite element volume conductor model. It was then applied as an extracellular potential to each node of each axon. The time step was set to 1 μs, which was equal to that used in the volume conductor model. Using the Brent optimization method, the minimum stimulus amplitude necessary to elicit action potential propagation in each axon was determined, as implemented in the SciPy optimization library [31]. The threshold isoline for a given stimulation amplitude was approximated by a fourth-order polynomial $P(y)$ using a least-squares fit. To determine the limits for volume integration, the roots a and b of $P(y)$ were calculated. The VTA was then calculated using the disk integration method evaluated between the two roots

$$V = \pi \int_{y=a}^{y=b} P^2(y) \mathrm{d}y \tag{10}$$

and subtracting the volume of the electrode geometry.

III. Results

For the approximation of the probabilistic voltage response and VTA, up to third-order multidimensional basis polynomials were chosen, as this polynomial orders has been accepted as an

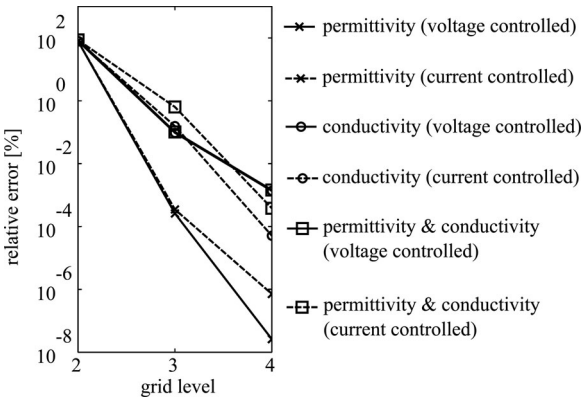

Fig. 3. *A posteriori* convergence of the variance of the RMS value of the representative probabilistic voltage response 1 mm from the active electrode contact for a random permittivity, random conductivity, and random permittivity as well as conductivity. Results are presented for voltage-controlled stimulation (solid lines) and current-controlled stimulation (dashed lines) with a parameter uncertainty of 20%.

appropriate approximation degree for various similar modeling problems [17]. According to (3), the number of polynomials was 10 for two random parameters and 35 for four random parameters. The resulting polynomial approximation of the probabilistic quantities was evaluated for 1 million uniformly distributed random samples for each parameter. This ensured that the probability density of the desired quantities was accurately represented. A smaller number of samples would also likely be sufficient. However, since the evaluation of the polynomial expansion is not computationally expensive, using a larger number of random samples than the minimum required is not critical regarding the computation time, but may increase the accuracy of the probabilistic properties of the desired quantities.

In a first step, the influence of the uncertainties in the material parameters of gray and white matter on the voltage response for current-controlled and voltage-controlled stimulations was investigated for three different cases, where the 1) conductivity; 2) permittivity; and 3) both conductivity and permittivity were modeled as probabilistic parameters. Since the probabilistic voltage response and VTA is approximated by a truncated series of random polynomials, the quality of this approximation was controlled by computing the relative error of the variance of the root mean square (RMS) value for the resulting voltage responses at different grid levels (see Fig. 3). Each study case showed a good convergence of the variance with a relative error below 1% at a grid level of 3 and 0.01% at a grid level of 4. At this grid level, 65 FEM computations were necessary for the studies in which only relative permittivity or conductivity was modeled as random parameters, and 401 FEM computations were required to capture the full set of random parameters.

In the case where conductivity as well as relative permittivity were modeled as random parameters, the resulting probabilistic voltage response showed almost the same waveform shape for the mean value as well as for the 0.025 and 0.975 quantiles (see Fig. 4). The uncertainty in the voltage response for current-controlled and voltage-controlled stimulations differed both in their relative magnitudes and probability density. While the probability for the voltage-controlled stimulation resembled a more symmetric density, the density for current-controlled stimulation was strongly asymmetric leading to a larger uncertainty in the voltage response above the mean value. In addition, the magnitude of the uncertainty for current-controlled stimulation was higher than for voltage-controlled stimulation. To investigate the influence of the uncertainties of the voltage response in the proximity of the electrode contact, the average uncertainty of the RMS amplitude of the voltage response within a distance of 2.5 mm to the active electrode contact in the coronary plane was computed. In the cases, where the conductivity was modeled as a random parameter, the uncertainties in the voltage response for current-controlled stimulation was almost as large as the parameter uncertainties. In contrast, when only the relative permittivity was modeled as a random parameter, the uncertainty in the probabilistic voltage response was negligible for voltage-controlled stimulation. For current-controlled stimulation, the uncertainty in the voltage response was slightly larger, but remained below 1% for a parameter uncertainty of 20%. Accordingly, the uncertainties in the voltage response with random conductivity and random relative permittivity showed almost the same results as the study, in which only the conductivity was modeled as a random parameter (see Table III). Therefore, further investigations on the influence of different magnitudes of uncertainties in the parameters on the voltage response and the neural activation were carried out for the conductivity modeled as a random parameter, while the relative permittivity remained at the mean value. Regarding the voltage response, different magnitudes of 10% and 40% of the parameter uncertainty in the random conductivity showed similar results of almost halved and doubled uncertainties compared to the values obtained for a parameter uncertainty of 20%.

Using the results from the presented study cases for the uncertainty of the probabilistic voltage response for current-controlled and voltage-controlled stimulations, the probabilistic VTA was computed for gray and white matter, modeled as random parameters with a relative standard deviation of 10%, 20%, and 40%. Similar to the investigation of the uncertainty of the probabilistic voltage response, the relative error of the variance of the VTA was investigated for different grid levels to ensure a relative error below 1% (see Fig. 5). In contrast to the investigation of the probabilistic voltage response, the convergence rate decreased for the variance of the VTA. Therefore, it was necessary to increase the grid level for the voltage-controlled cases with a relative standard deviation of 10% and 20% to ensure the given relative error bound. The resulting number of necessary FEM computations and computation of the VTA varied between 29 variants for a grid level of 3 and 145 variants for a grid level of 5. The resulting probabilistic volumes of tissue activated showed larger uncertainties for current-controlled stimulation than for voltage-controlled stimulation as already noted in the probabilistic voltage response (see Fig. 6).

For a parameter uncertainty of 20%, the relative standard deviation of the VTA is approximately 32% for current-controlled stimulation and 14% for voltage-controlled stimulation. It increases for a parameter uncertainty of 40% up to 84% and 31%, respectively (see Table IV). In addition to the result that

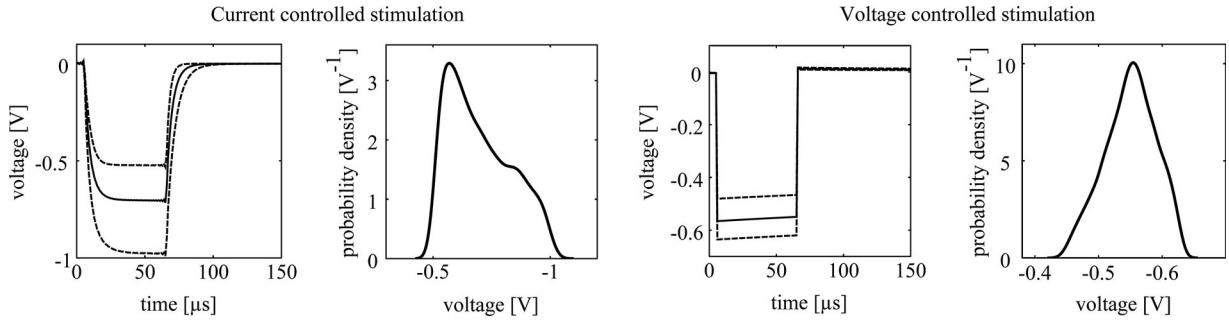

Fig. 4. Representative probabilistic voltage response 1 mm from the active electrode contact (left) and probability density of the shown voltage response at a time step of 64 μs (right) for a current- and voltage-controlled stimulations of -1 V and -1 mA, respectively. The mean voltage response (solid line) as well as 0.025 and 0.975 quantile (dashed line) for random conductivity and permittivity with a relative standard deviation of 20% are shown.

TABLE III
RMS UNCERTAINTY AND STANDARD DEVIATION OF THE PROBABILISTIC VOLTAGE RESPONSE WITHIN 2.5-mm DISTANCE TO THE ACTIVE ELECTRODE CONTACT COMPUTED AT THE MEAN AXON NODES IN THE CORONARY PLANE

parameter	parameter uncertainty [%]	voltage response uncertainty [%]	
		voltage cont.	current cont.
κ & ε_r	20	7.2 ± 0.3	18.4 ± 0.3
κ	20	7.2 ± 0.3	18.3 ± 0.3
ε_r	20	0.0 ± 0.0	0.7 ± 0.0
κ	10	3.6 ± 0.1	8.8 ± 0.2
κ	40	15.7 ± 0.7	43.8 ± 1.0

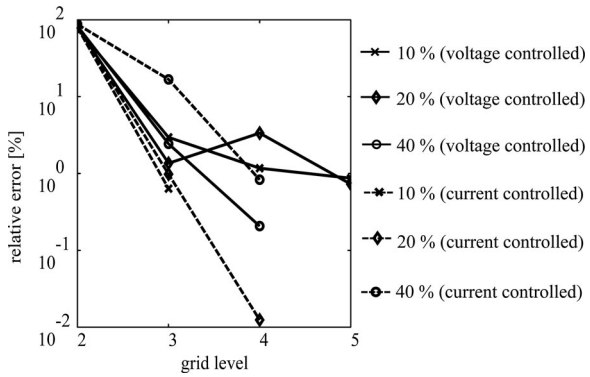

Fig. 5. *A posteriori* convergence of the variance of the probabilistic VTA for random conductivity with uncertainties of 10%–40% for voltage-controlled (-1.5 V) and current-controlled (-1.5 mA) stimulations. Refinement of the solution by increasing the grid level was stopped when the relative error was below 1%.

the uncertainties in the VTA were larger for current-controlled stimulation than for voltage-controlled stimulation, the magnitude of the uncertainties in the VTA almost doubled compared to the uncertainties in the voltage response for both stimulation cases (see Tables III and IV). The overall shape and characteristics of the probability densities of the VTA for current-controlled and voltage-controlled stimulations resembled those of the voltage response leading to a strongly asymmetric probability density for current-controlled stimulation and an almost symmetric probability density for voltage-controlled stimulation (see Fig. 7). Therefore, for current-controlled stimulation, larger VTAs are more probable than smaller VTAs compared to the mean value. Although the values for the 0.025 and 0.975 quantiles of the VTA increase for larger stimulation amplitudes ranging from approximately 135 to 383 mm^3 for a stimulation amplitude of -1.5 mA, the relative standard deviation remains almost constant for the different stimulation amplitudes (see Fig. 7).

IV. DISCUSSION

Based on the uncertainties in the material properties of brain tissue, which were modeled as random uniform variables, the probabilistic voltage response and VTA for voltage- and current-controlled stimulations were computed in a finite element model of the human brain coupled with a multicompartmental nerve fiber model. The results suggest that the uncertainty in the material parameters of brain tissue can have a substantial effect on the estimated time-dependent voltage response in the proximity of the stimulated target as well as on the predicted VTA. Both quantities were influenced more by the probabilistic conductivity than probabilistic permittivity. A small influence of the relative permittivity on the voltage response as well as on the VTA in DBS for current-controlled stimulation was also reported in a previous parameter study [32]. However, the mentioned parameter study was limited to the investigation of a halved and doubled relative permittivity value in a homogeneous analytical model and did not consider uncertainties in the material properties of brain tissue to quantify the effect of the relative permittivity on its own. The results of this study suggest that for voltage-controlled stimulation the influence of uncertainties in the relative permittivity of brain tissue are even smaller than in current-controlled stimulation and that for both stimulation types these uncertainties are negligible in volume conductor models of DBS. This effect is assumed to result from a domination of the real part of the complex conductivity compared to the imaginary part, which represents the capacitive properties of the brain tissue [33]. Modeling of the conductivity and relative permittivity of brain tissue as probabilistic parameters revealed an asymmetric probability distribution of the probabilistic voltage response for current-controlled stimulation (see Fig. 4). This asymmetry results from the inversely proportional dependence of the voltage response on the applied stimulation current as stated in Ohm's law. For voltage-controlled stimulation, the probability density of the voltage response resembled a more symmetric distribution, which results from the influence of the electrical double layer, which is formed around the active

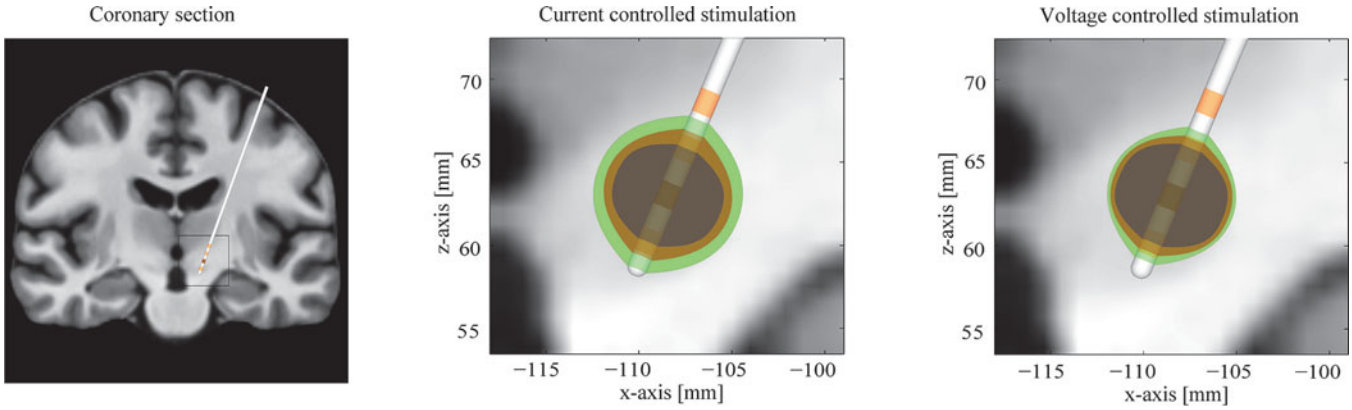

Fig. 6. Coronary section of the MRI dataset with the DBS electrode and the ROI overlayed with the probabilistic VTA for current-controlled stimulation (−1.5 mA) and voltage-controlled stimulation (−1.5 V). The mean VTA (orange), 0.025 quantile (dark blue), and 0.975 quantile (green) for random conductivity with a relative standard deviation of 20% are shown.

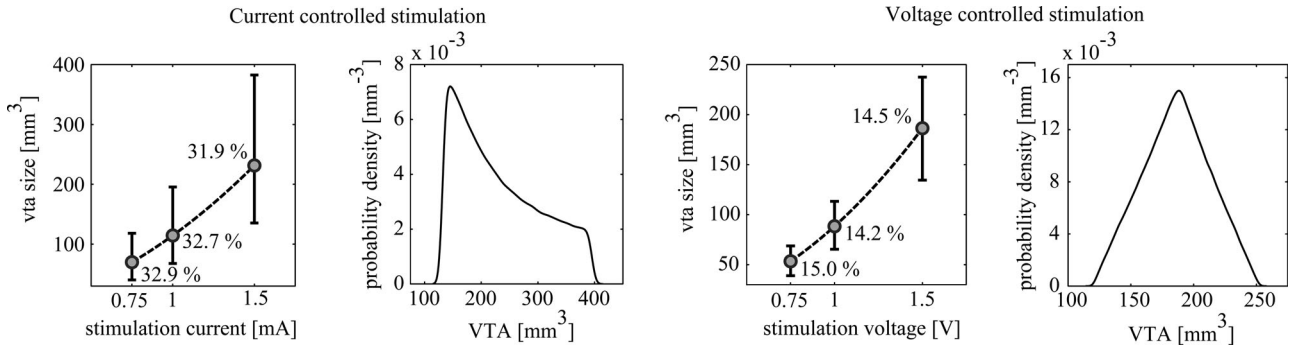

Fig. 7. Probabilistic VTA (left) and the corresponding probability density (right) at a stimulation amplitude of −1.5 mA and −1.5 V for current-controlled and voltage-controlled stimulations, respectively. Mean value, 0.025 quantile, 0.975 quantile, and relative standard deviation of the VTA for a random conductivity with a uncertainty of 20% are shown.

electrode contact in this stimulation setup [6]. The electrical double layer is represented here as a constant phase element, which acts as a voltage divider and, therefore, reduces the influence of uncertainties in the material parameters. Consequently, the absence of the influence of the electrical double layer in current-controlled stimulation should lead to a more direct influence of the uncertainty in the material properties of brain tissue on the voltage response in the proximity of the stimulated target. This is in agreement with the magnitudes of the computed uncertainties in the probabilistic voltage response compared to the those of the predefined uncertainties in the material properties (see Table III). However, for a parameter uncertainty of 40% the relative standard deviation of the probabilistic voltage response for current-controlled stimulation was approximately 43.8% ± 1.0% and, therefore, slightly larger than the parameter uncertainty. To exclude approximation errors, the relative standard deviation of the probabilistic voltage response was also computed for an increased grid level of 5 and a polynomial degree of up to 7, which resulted in a change of only 0.1%. Therefore, it is assumed that this effect results from the inversely proportional dependence of the voltage response on the applied stimulation current, as discussed above.

The proposed method approximates the stochastics of the desired quantities, the voltage response and VTA, by a multidimensional polynomial expansion. The coefficients of this

TABLE IV
UNCERTAINTY OF THE VTA FOR RANDOM CONDUCTIVITIES OF GRAY AND WHITE MATTER FOR VOLTAGE-CONTROLLED (−1.5 V) AND CURRENT-CONTROLLED (1.5 mA) STIMULATIONS

parameter uncertainty [%]	volume of tissue activated uncertainty [%]	
	voltage cont.	current cont.
10	7.1	14.0
20	14.5	31.8
40	30.7	84.0

polynomial expansion are computed by a multidimensional integration scheme based on Smolyak sparse grids. To ensure a valid approximation of the stochastics, it is necessary to check their convergence for increasing number of integration points depending on the chosen grid level. Therefore, the relative error of the variance of the desired quantities was controlled for increasing grid levels. The relative error for the probabilistic voltage response was below 1% for a grid level of 3 and below 0.1% for a grid level of 4, which suggest a good approximation of the probabilistic voltage response even for a grid level of 3 (see Fig. 3). The convergence of the polynomial approximation depends on the smoothness and functional dependences of the parameters on the desired quantity. Therefore, a smooth functional dependence without discontinuities is beneficial for the convergence rate of the polynomial approximation [17], which

is the case for the computation of the voltage response depending on the solution of the linear differential equation (9) with mixed Neumann and Dirichlet boundary conditions. However, the convergence for the approximation of the probabilistic VTA was worse compared to that of the probabilistic voltage response and showed a minor stability (see Fig. 5). Therefore, it was necessary to increase the grid level to 5 for the voltage-controlled cases with a relative standard deviation of 10% and 20% to ensure a relative error of below 1%. It is assumed, that this effect results from the nonlinear membrane dynamics of the multicompartmental model of the mammalian nerve fibers used to compute the neural activation in the proximity of the stimulated target [23]. The varying convergence rate for the different study cases resulted in varying numbers of necessary deterministic model computations, ranging from 29 computations for a grid level of 3 up to 145 computations for a grid level of 5. The total number of deterministic model computations for all study cases was 514 resulting in 64 764 computations of the thresholds necessary to elicit an action potential in the mammalian nerve fibers.

Despite the decreased convergence rate, the probability densities of the resulting probabilistic VTAs resembled those of the probabilistic voltage response for current-controlled and voltage-controlled stimulations (see Fig. 7). Consequently, the probabilistic VTA for current-controlled stimulation has an asymmetric probability density resulting in a larger probability for overestimated VTA sizes compared to the mean. The relative standard deviation of the VTA remains approximately constant for different stimulation amplitudes for current-controlled as well as for voltage-controlled stimulation. However, the values of the 0.025 and 0.975 quantiles of the VTA increase for larger stimulation amplitudes, which also increases the possible over- and underestimated area in which no neural stimulation is desired. The relative standard deviation of the VTA almost doubled compared to that of the probabilistic voltage response, which is assumed to be an effect of the nonlinear membrane dynamics of the mammalian nerve fibers (see Fig. 4). Larger relative fluctuations of the VTA compared to the change in the conductivity of brain tissue were also reported for voltage-controlled stimulation in an *in silico* study in which the same axon model was used for the computation of the VTA [5]. For current-controlled stimulation, the extend of the VTA varied by up to 2 mm for a stimulation amplitude of -1.5 mA and a parameter uncertainty of 20% (see Fig. 6). This predefined parameter uncertainty is located in the lower value set of parameter uncertainty found in the experimental literature (see Table I). The stimulated target, the STN, has a diameter of approximately 10–15 mm [34] and can be classified in a limbic, associative, and motoric domain [35], which have different effects on the motor symptoms of PD when stimulated [22]. Therefore, the results of this study suggest that even small changes of the electrical conductivity in volume conductor models of DBS can have a relevant influence on the computed therapeutical effect, especially for current-controlled stimulation. Although uncertainty in the VTA for voltage-controlled stimulation was smaller than for current-controlled stimulation, impedance changes in voltage-controlled stimulation could result in a substantial change of the VTA over time. Measurements of the electrode impedance in an *in vivo* study performed in nonhuman primates showed a substantial change of the impedance and voltage distribution of approximately 50% for voltage-controlled stimulation and only approximately 7% for current-controlled stimulation after 60 min of stimulation [3]. This result suggests that the VTA for current-controlled stimulation would remain more constant over time while the VTA for voltage-controlled stimulation would change substantially over time. To date, first clinical trials report an improvement of symptoms in PD with current-controlled DBS, but a comparison between the effects of current-controlled and voltage-controlled stimulations in humans is still pending [36].

The used method to compute the VTA in the proximity of the stimulated target is a well-established procedure to receive a first estimation of the therapeutical effect of DBS [5], [6], [8]. Nevertheless, the method simplifies reality by predefining a perpendicular alignment of the neurons relative to the electrode body while gray matter neurons have a more deviating orientation [37]. In addition, uncertainty in the VTA could be affected by the axon fiber diameter, which may vary in the proximity of the DBS electrode for different stimulated targets. Considering an uncertainty in the fiber diameter and internodal spacing, the proposed method would allow to quantify this uncertainty. Since only thresholds necessary for eliciting an action potential in each neuron are computed, no insights about the complex network effects in the basal ganglia can be gained. To have a realistic representation of the spatial distribution of gray matter, white matter, and cerebrospinal fluid in the brain, the volume conductor model used in this study is based on segmented MRI data from a digital brain atlas, which consists of the average image data of 24 humans [20]. While the information of the segmented MRI data agrees well with the overall anatomy of the brain, the data does not fully render the basal ganglia nuclei, resulting in homogeneous white matter areas at the stimulation target, which consist anatomically of gray matter. Therefore, a computation of the VTA by a rotation integral was chosen, since it was assumed that the local effect of tissue heterogeneity at the stimulation target is small. A more realistic representation of the basal ganglia nuclei could improve the results and the investigation of tissue heterogeneity in this area. However, a preferably precise segmentation of the basal ganglia nuclei is made problematic, since high-resolution data, expert advices, and manual segmentation steps are necessary [21]. The material properties of gray and white matter were modeled as uniform distributions. Because literature data of these parameters are scarce, a uniform distribution having a maximum entropy probability distribution is suitable to model some kind of a "worst case" scenario and more data would be needed to gain a more realistic representation of their uncertainty. If a large number of data measurements with the same experimental setup could be available, a normal distribution of the data would be most likely. Since the focus was on the uncertainties in the material properties of the brain tissue in the proximity of the stimulated target, possible uncertainties in the material properties of cerebrospinal fluid were not included in this study. However, for applications, were the stimulated target is closer to areas of cerebrospinal fluid, such as the ventricles, the influence of these uncertainties could be of

interest. The polynomial expansion of the probabilistic voltage response and VTA was computed for up to third-order polynomials. It was ensured that this polynomial degree is sufficient to present the stochastics of these quantities with a relative error of below 1%. However, for nonuniform parameter distributions and more complex functional dependences, such as strong nonlinearities, a higher polynomial degree would be necessary. Since the quality of the approximation by a certain polynomial degree depends on the number of grid points for the numerical integration of the coefficients of the polynomial approximation, a larger grid level would be necessary to ensure convergence of the stochastics.

Despite the discussed simplifications, the proposed method enables a first estimation and error bounds of the extend of uncertainties in the voltage response and neural activation in volume conductors of DBS to be computed with relative computational efficiency. The number of computations of the deterministic model to obtain the probabilistic VTAs ranged from 29 to 145 for two uncertain parameters, which are substantially less computations compared to a classical MCS. If the number of parameters increase, a classical MCS might be a more efficient way. However, performing a classical MCS on the computational expensive finite element model in a reasonable time would be challenging. The reduction of the necessary deterministic model computations is achieved not only by using orthogonal projections to compute the coefficients of the polynomial approximations, but also by using sparse grids for the numerical evaluation of the coefficients. These sparse grids are nested, which means that a grid of a certain level n contains also the solution for any smaller grid and, therefore, provides a convenient way of ensuring the convergence of the approximation. Furthermore, already computed grid points can be used for a refinement of the solution. The proposed method does not require a modification of the underlying deterministic model. Therefore, the method can be applied to other models subject to uncertainties in the model parameters.

V. Conclusion

In this study, the influence of uncertainties in the material properties of brain tissue on the uncertainty in the probabilistic voltage response and VTA during DBS was investigated. The results suggest that the major contribution to the uncertainty of the desired quantities arises from uncertainties in the conductivity. The contribution of uncertainties in the relative permittivity was found to be negligible. Small uncertainties in the conductivity approximately doubled the level of uncertainty in the probabilistic VTA. These results lead to the conclusion that the uncertainty in the conductivity of brain tissue should be considered in volume conductor models of DBS and points out the limitations of deterministic models by providing only a single solution. The proposed method to compute the probabilistic desired quantities was found to be computationally efficient for up to four parameters, requiring a substantially smaller amount of deterministic model evaluations than a traditional probabilistic sampling method, such as MCS. Depending on the model problem and required accuracy, using the proposed method the quantification of uncertainty for additional parameters, such as the electrical double layer and electrode geometry, may also be possible.

Acknowledgment

The authors wish to acknowledge the Research IT Service at University College Dublin and the SFI/HEA Irish Centre for High-End Computing (ICHEC) for providing HPC resources that have contributed to the research results reported within this paper.

References

[1] A. L. Benabid, "Deep brain stimulation for Parkinson's disease," *Curr. Opin. Neurobiol.*, vol. 13, pp. 696–706, 2003.

[2] (2012, Jun. 13). *Products and Procedures for Medtronic Deep Brain Stimulation.* [Online]. Available: http://professional.medtronic.com/pt/neuro/dbs-md/prod/index.htm

[3] S. F. Lempka, M. D. Johnson, S. Miocinovic, J. L. Vitek, and C. C. McIntyre, "Current-controlled deep brain stimulation reduces *in vivo* voltage fluctuations observed during voltage-controlled stimulation," *Clin. Neurophysiol.*, vol. 121, pp. 2128–2133, 2010.

[4] M. C. Rodriguez-Oroz, M. Rodriguez, J. Guridi, K. Mewes, V. Chockkman, J. L. Vitek, M. R. DeLong, and J. A. Obeso, "The subthalamic nucleus in Parkinson's disease: Somatotopic organization and physiological characteristics," *Brain*, vol. 124, pp. 1777–1790, 2001.

[5] C. R. Butson, C. B. Maks, and C. C. McIntyre, "Sources and effects of electrode impedance during deep brain stimulation," *Clin. Neurphysiol.*, vol. 117, pp. 447–454, 2006.

[6] P. F. Grant and M. M. Lowery, "Effect of dispersive conductivity and permittivity in volume conductor models of deep brain stimulation," *IEEE Trans. Biomed. Eng.*, vol. 57, no. 10, pp. 2386–2393, Oct. 2010.

[7] C. C. McIntyre, W. Grill, D. L. Sherman, and N. V. Thakor, "Cellular effects of deep brain stimulation: Model-based analysis of activation and inhibition," *J. Neurophysiol.*, vol. 91, pp. 1457–1469, 2004.

[8] N. Yousif and X. Liu, "Investigating the depth electrode-brain interface in deep brain stimulation using finite element models with graded complexity in structure and solution," *J. Neurosci. Methods*, vol. 184, no. 1, pp. 142–151, Oct. 2009.

[9] S. Gabriel, R. W. Lau, and C. Gabriel, "The dielectric properties of biological tissues—Part III: Parametric models for the dielectric spectrum of tissues," *Phys. Med. Biol.*, vol. 41, no. 11, pp. 2271–2293, Nov. 1996.

[10] L. Geddes and L. Baker, "The specific resistance of biological material—A compendium of data for the biomedical engineer and physiologist," *Med. Biol. Eng.*, vol. 5, no. 3, pp. 271–293, May 1967.

[11] K. R. Foster and H. P. Schwan, "Dielectric properties of tissues and biological materials: A critical review," *Crit. Rev. Biomed. Eng.*, vol. 17, no. 1, pp. 25–104, 1989.

[12] J. Latikka, T. Kuurne, and H. Eskola, "Conductivity of living intracranial tissues," *Phys. Med. Biol.*, vol. 46, no. 6, pp. 1611–1616, Jun. 2001.

[13] C. Gabriel, A. Peyman, and E. H. Grant, "Electrical conductivity of tissue at frequencies below 1 MHz," *Phys. Med. Biol.*, vol. 54, pp. 4863–4878, 2009.

[14] D. Xiu, *Numerical Methods for Stochastic Computations: A Spectral Method Approach*. Princeton, NJ: Princeton Univ. Press, 2010.

[15] H. Osnes and S. Joakim, "Uncertainty analysis of ventricular mechanics using the probabilistic collocation method," *IEEE Trans. Biomed. Eng.*, vol. 59, no. 8, pp. 2171–2179, Aug. 2012.

[16] J. S. Preston, T. Tasdizen, C. M. Terry, A. K. Cheung, and M. K. Robert, "Using the stochastic collocation method for the uncertainty quantification of drug concentration due to depot shape variability," *IEEE Trans. Biomed. Eng.*, vol. 56, no. 3, pp. 609–620, Mar. 2009.

[17] B. Sudret, M. Berveiller, and M. Lemaire, "A stochastic finite element procedure for moment and reliability analysis," *Eur. J. Comput. Mech.*, vol. 15, pp. 825–866, 2006.

[18] L. Nechak, S. Berger, and E. Aubry, "Non-intrusive generalized polynomial chaos approach to the stability analysis of uncertain nonlinear dynamic systems," in *Proc. 8th Int. Multi-Conf. Syst. Signals Dev.*, 2011, pp. 1–6.

[19] F. Nobile, R. Tempone, and C. G. Webster, "A sparse grid stochastic collocation method for partial differential equations with random input data," *SIAM J. Numer. Anal.*, vol. 46, no. 5, pp. 2309–2345, May 2008.
[20] T. Rohlfing, N. M. Zahr, E. V. Sullivan, and A. Pfefferbaum, "The SRI24 multi-channel brain atlas," *in Proc. Soc. Photo Opt. Instrum. Eng.*, 2008, vol. 6914, pp. 691409-1–691409-12.
[21] C. Schmidt and U. van Rienen, "Modeling the field distribution in deep brain stimulation: The influence of anisotropy of brain tissue," *IEEE Trans. Bio-Med. Eng.*, vol. 59, no. 6, pp. 1583–1592, Jun. 2012.
[22] K. A. Follett, F. M. Weaver, M. Stern, K. Hur, C. L. Harris, P. Luo, W. J. J. Marks, J. Rothlind, O. Sagher, C. Moy, R. Pahwa, K. Burchiel, P. Hogarth, E. C. Lai, J. E. Duda, K. Holloway, A. Samii, S. Horn, J. M. Bronstein, G. Stoner, P. A. Starr, R. Simpson, G. Baltuch, A. De Salles, G. D. Huang, and D. J. Reda, "Pallidal versus subthalamic deep-brain stimulation for Parkinson's disease," *New Engl. J. Med.*, vol. 362, pp. 2077–2091, 2010.
[23] C. C. McIntyre, A. G. Richardson, and W. M. Grill, "Modeling the excitability of mammalian nerve fibers: Influence of afterpotentials on the recovery cycle," *J. Neurophysiol.*, vol. 87, no. 2, pp. 995–1006, Feb. 2002.
[24] M. S. Eldred, C. G. Webster, and P. G. Constantine, "Evaluation of non-intrusive approaches for Wiener–Askey generalized polynomial chaos," presented at the 10th AIAA Nondetermin. Approach. Conf., Apr. 2008, Paper AIAA-2008-1892.
[25] S. H. Lee and W. Chen, "A comparative study of uncertainty propagation methods for black-box-type problems," *Struct. Multidisc. Optim.*, vol. 37, no. 3, pp. 239–253, Jan. 2009.
[26] J. Waldvogel, "Fast construction of the Fejér and Clenshaw–Curtis quadrature rules," *BIT Numer. Math.*, vol. 46, pp. 195–202, 2006.
[27] C. Schmidt and U. van Rienen, "Quantification of uncertainties in brain tissue conductivity in a heterogeneous model of deep brain stimulation using a non-intrusive projection approach," in *Proc. IEEE 34th Annu. Int. Conf. Eng. Med. Biol. Soc.*, Aug./Sep. 2012, pp. 4136–4139.
[28] C. R. Butson and C. C. McIntyre, "Tissue and electrode capacitance reduce neural activation volumes during deep brain stimulation," *Clin. Neurophysiol.*, vol. 116, pp. 2490–2500, 2005.
[29] X. F. Wei and W. M. Grill, "Impedance characteristics of deep brain stimulation electrodes *in vitro* and *in vivo*," *J. Neural. Eng.*, vol. 6, pp. 046008-1–046008-9, 2009.
[30] M. L. Hines and N. T. Carnevale, "The neuron simulation environment," *Neur. Comput.*, vol. 9, no. 6, pp. 1179–209, Aug. 1997.
[31] E. Jones, T. Oliphant, P. Peterson *et al.*, "SciPy: Open source scientific tools for python," 2001. Available: http://www.scipy.org
[32] C. A. Bossetti, M. J. Birdno, and W. M. Grill, "Analysis of the quasi-static approximation for calculating potentials generated by neural stimulation," *J. Neur. Eng.*, vol. 5, pp. 44–53, 2008.
[33] R. Plonsey and D. B. Heppner, "Considerations of quasi-stationarity in electrophysiological systems," *B Math. Biophys.*, vol. 29, pp. 657–664, 1967.
[34] M. S. Okun, H. H. Fernandez, S. S. Wu, L. Kirsch-Darrow, D. Bowers, F. Bova, M. Suelter, C. E. Jacobson, X. Wang, C. W. Gordon, P. Zeilman, J. Romrell, P. Martin, H. Ward, R. L. Rodriguez, and K. D. Foote, "Cognition and mood in Parkinson's disease in subthalamic nucleus versus globus pallidus interna deep brain stimulation: The COMPARE trial," *Ann. Neurol.*, vol. 65, pp. 586–595, 2009.
[35] C. Guigoni, Q. Li, I. Aubert, S. Dovero, B. H. Bioulac, B. Bloch, A. R. Crossman, C. E. Gross, and E. Bezard, "Involvement of sensorimotor, limbic, and associative basal ganglia domains in L-3,4-dihydroxyphenylalanine-induced dyskensia," *J. Neurosci.*, vol. 25, pp. 2912–2107, 2005.
[36] M. S. Okun, B. V. Gallo, G. Mandybur, J. Jagid, K. D. Foote, F. J. Revilla, R. Alterman, J. Jankovic, R. Simpson, F. Junn, L. Verhagen, J. E. Arle, B. Ford, R. R. Goodman, R. M. Stewart, S. Horn, G. H. Baltuch, B. H. Kopell, F. Marshall, D. Peichel, R. Pahwa, K. E. Lyons, A. I. Tröster, J. L. Vitek, and M. Tagliati, "Subthalamic deep brain stimulation with a constant-current device in Parkinson's disease: An open-label randomised controlled trial," *Lancet Neurol.*, vol. 11, pp. 140–149, 2012.
[37] M. Axer, K. Amunts, D. Grässel, J. Dammer, H. Axer, U. Petrzyk, and K. Zilles, "A novel approach to the human connectome: Ultra-high resolution mapping of fiber tracts in the brain," *NeuroImage*, vol. 54, pp. 1091–1101, 2011.

Christian Schmidt (S'12) received the First State Examination degree in mathematics, physics, and informatics from the University of Rostock, Rostock, Germany, in 2009, where he is currently working toward the Ph.D. degree in bioelectrical engineering.

From 2009 to 2010, he was a Scientific Assistant at the Institute of Physics, University of Rostock. In 2010, he qualified for a doctoral scholarship in the Research Training Group "welisa" at the Institute of General Electrical Engineering, University of Rostock. His research interests include application of algorithms for modeling and simulation of deep brain stimulation.

Peader F. Grant (M'05) received the B.E. and Ph.D degrees from the School of Electrical, Electronic and Mechanical Engineering, University College Dublin, Dublin, Ireland, in 2008 and 2011, respectively.

He was appointed to the staff in University College Dublin as a Lecturer in 2011. His research focuses on computational electromagnetic and neural models of the effects of deep brain stimulation as a therapy for Parkinsons Disease. Since 2006, he has authored several international journal and international conference publications.

Madeleine Lowery (M'00) received the B.E. and Ph.D. degrees from the Department of Electronic and Electrical Engineering, University College Dublin, Ireland, in 1996 and 2000, respectively.

She is a Senior Lecturer in the School of Electrical, Electronic, and Communications Engineering, University College Dublin, Dublin, Ireland. Her research involves the exploration of nerve and muscle activity through mathematical modeling, analysis, and experimentation, to increase understanding of neuromuscular activity in healthy and diseased states and develop novel and improved rehabilitation strategies. Her research interests include electromyography, myoelectric prosthetic control, bioelectromagnetics, electrical stimulation, deep brain stimulation and neural control of movement. Between 2000 and 2005, he was a Postdoctoral Fellow then Research Assistant Professor at the Rehabilitation Institute of Chicago and the Department of Physical Medicine and Rehabilitation, Northwestern University.

Dr. Lowery is a Member of the Council of the International Society of Electrophysiology and Kinesiology (ISEK).

Ursula van Rienen (M'01) received the diploma in mathematics in 1983 from the University of Bonn, Germany, and the Ph.D. degree in mathematics and scientific computing in 1989 from the Darmstadt University of Technology (TUD), Germany.

In 1997, she finished her habilitation (the "second book") and received the venia legendi for the fields *Electromagnetic Field Theory* and *Scientific Computing* from the Faculty of Electrical Engineering and Information Technology at the TUD. Since October 1997, she holds the chair in "Electromagnetic Field Theory" at the University of Rostock, Germany. Her research work is focussed on computational electromagnetics with various applications, ranging from biomedical engineering to accelerator physics.